

Percolative conductivity in alkaline earth silicate melts and glasses

M. Malki[†], M. Micoulaut[‡], F. Chaimbault[†], Y. Vaills[†], P. Simon[†]

[†] *CRMHT-CNRS 1D, avenue de la Recherche Scientifique*

45071 Orléans Cedex 02, France

Université d'Orléans, 45067 Orléans Cedex 02, France

[‡] *Laboratoire de Physique Théorique des Liquides Université Pierre et Marie Curie*

Boite 121 4, Place Jussieu, 75252 Paris Cedex 05, France

(October 30, 2018)

Ion conducting $(CaO)_x(SiO_2)_{1-x}$ glasses and melts show a threshold behaviour in dc conductivity near $x = x_t = 0.50$, with conductivities increasing linearly at $x > x_t$. We show that the behaviour can be traced to a rigid ($x < 0.50$) to floppy ($x > 0.50$) elastic phase transition near $x = x_t$. In the floppy phase, conductivity enhancement is traced to increased mobility or diffusion of Ca^{2+} carriers as the modified network elastically softens.

Pacs: 61.43Fs-62.20.-x

Electrical and thermal properties are directly related to the structure of silicate melts and investigations into their structure have received therefore considerable attention in earth science. It is indeed of fundamental importance to understand how magmas which contain alkali and alkaline earth silicates behave under different physical circumstances. Alkali silicate glasses have been extensively studied within this context and numerous articles have focused on the variation of structure [1], conductivity [2], glass transition [3], etc. with respect to the alkali concentration. On the other hand, a small number of studies on alkaline earth silicate glasses have been reported to date. Some of them, however, have focused either on the structure of glasses containing barium and calcium silicates [4], or on the thermodynamics and miscibility of the corresponding melts [5] and density or specific volume [6]. It is worth mentioning that most of these studies have been restricted around the 50% concentration of alkaline earth oxide where glass-forming tendency (GFT) is optimized [7]. Finally, even though most of the fast ionic conductors (FIC) [8,9] having potential applications in electrochemical devices such as solid state batteries are alkali (or silver) silicates or thiosilicates, the conductivity of alkaline earth silicates is non-negligible [about $2.10^{-7} \Omega^{-1}.cm^{-1}$ at $550^{\circ}C$] and the role of the migrating calcium cations remains to be completely understood. Our work attempts to address for the first time this basic issue.

In this Letter, we report on $(CaO)_x(SiO_2)_{1-x}$ glasses and the common physical origin for the behavior in both the GFT and the conductivity data that follow directly from the Phillips-Thorpe constraint theory [10]. Calcium silicate melts and glasses near $x = 0.5$ are optimally constrained and display percolative conduction in both melts and glasses. This is a new feature that has never been observed in the corresponding alkali silicates, which links ionic conductivity to glass elasticity and structure. Furthermore, we show that the sudden increase of the conductivity at high calcium concentration has to be a consequence of the calcium cation mobility percolation arising from the floppy to rigid transition [11]. The major consequence is that here the carrier concentration does not dominate the conductivity, as usually reported.

The samples were prepared by mixing pre-dried SiO_2 (99.99 %) and $CaCO_3$ (99.95 %)

powders in the correct proportions. For each sample, the mixture was melted in a platinum crucible at 1650°C for two hours, and quenched by plunging the bottom of the crucible in cold water. The glass transition temperatures were determined with a differential scanning calorimeter Setaram DSC-1600 at a heating rate $10^{\circ}\text{C}/\text{min}$. These values are slightly larger than those reported by Shelby [12] using the dilatometric technique but they exhibit the same global trend (fig. 1), i.e. a plateau up to a Calcium concentration in the range $[0.45-0.48]$ and a more or less linear increase for higher concentrations. In the solid state, the complex electrical conductivity was measured with an impedance spectrometer 4194A in the temperature range $500^{\circ}\text{C} - 950^{\circ}\text{C}$ and in the frequency range 100 Hz-10 MHz. The samples were 0.5 cm^2 glass pellets with a thickness about 1 mm . Platinum was evaporated as electrodes on both faces of the pellet. The temperature was measured with a Pt/Pt-10%Rh thermocouple located at about 1 mm from the sample [13]. We restricted our study in the molten state to only three compositions.

The dc conductivity σ displays almost the same trend as $T_g(x)$, with a very small value (about $10^{-7}\text{ }\Omega^{-1}.\text{cm}^{-1}$) for $x < 0.47$ and a sudden increase for larger compositions. The almost constant value of σ in the low calcium region and the sudden increase for $x > 0.47$ has been also obtained in simulations and experiments for the molten state (fig. 2, insert [14]), suggesting that molten and glassy state behave similarly. Furthermore, we have observed the same kind of trend in our molten samples (see fig. 3, below) which are almost at the same temperatures than those of Ref. [14]. Figure 3 shows the Arrhenius plots $[\sigma T = \sigma_0 \exp[-E_A/k_B T]]$ of the conductivity σ for the glassy and the molten state. From the latter, it is also obvious that the conductivity data of three compositions in the $x \leq 0.50$ range map onto each other and have the same global trend in the glass.

These results can be quantitatively understood using the tools of Lagrangian bonding constraints as introduced by Phillips [10]. A network constrained by bond-stretching and bond-bending forces sits indeed at a mechanically critical point when the number of constraints per atom n_c equals the network dimensionality. At this point, glass optimum is attained and GFT is enhanced [15]. These ideas can be cast in terms of percolation theory

by evaluating the number of zero frequency modes (floppy modes F/N) from a dynamical matrix [11], which vanish at the floppy to rigid transition. The very accurate agreement of experiments in chalcogenides with the predictions of the theory is quite remarkable [16,17] but further investigations devoted to alkali oxide glasses have been performed only recently [18,19].

We consider the $CaO-SiO_2$ system as a network of N atoms composed of n_r atoms that are r -fold coordinated. Enumeration of mechanical constraints gives for bond-stretching forces $r/2$ and for bond-bending forces $(2r-3)$ constraints. The average number of floppy modes per atom F/N in a three-dimensional network is given by [11]:

$$F/N = n_d - n_c = 3 - \frac{1}{N} \sum_{r \geq 2} n_r \left(\frac{5r}{2} - 3 \right) \quad (0.1)$$

which applied to the present $(CaO)_x(SiO_2)_{1-x}$ case, yields:

$$F/N = 3 - \frac{11 - 7x}{3 - x} \quad (0.2)$$

provided that Si is four-folded and calcium and oxygen are two-fold coordinated. The coordination number used in equ. (0.2) for Ca deserves some comments since computer simulations [14] and EXAFS studies [20] have suggested that the number of nearest neighbors of the calcium atom may be about 6. However, Debye-Waller factor in these studies on combined systems using either BaO or CaO as network modifier are slightly different, suggesting that the oxygen neighbors of Ca were not all equivalent [20] thus promoting the chemical hypothesis for the coordination number of Ca ($r = 2$). On the other hand, in constraint theory one deals only with the bonds that provide a strong mechanical constraint, which means that the covalent bonds are the most qualified. To be more specific, one can use Pauling's definition to determine the fractional ionic character f in the $Ca-O$ bond [22], which yields here the value $f = 0.774$ and a corresponding covalency factor of 0.226. With a coordination of 6 for Ca , the corresponding covalent coordination is 1.36, somewhat lower than 2. Furthermore, mechanical constraints provided by alkali atoms connected to more than one oxygen have been suggested to be only resonating constraints [19], which do not

participate in the global counting. Finally, alkali silicate and tellurate glasses are illustrative precedents [18]. In these systems, the floppy to rigid transition occurs at the expected critical concentration [21] only if the involved atoms (Na) have a covalent coordination number of 1 (and the “Pauling” analysis [23] yields the covalent coordination $0.832 - 1.04$), even though the number of nearest neighbors [24] of the sodium atom is believed to be 5.

Our interpretation of the dc conductivity is as follows. At $x = x_c = 0.5$, the number of floppy modes F/N vanishes and the network undergoes a rigid to floppy transition, following equ. (0.2). For $x < 0.5$ the system is stressed rigid, i.e. there are more constraints than degrees of freedom. As a consequence, the mobility of the calcium cation is very weak because the cation has to overcome a strong mechanical deformation energy to move from one anionic site to another. In an ideal floppy glass at $x > 0.5$ where only bond-bending and bond-stretching forces are considered [10] this deformation energy is zero and related elastic constants (c_{11} , c_{44}) vanish [25]. Therefore, percolation of floppiness equals percolation of Ca mobility. As a result, one has a substantial increase of the mobility hence of the conductivity. In the strong electrolyte Anderson-Stuart model [26], the activation energy for conductivity $E_A = E_C + E_m$ depends on the Coulombic term E_C (which controls the carrier rate) and a strain term E_m related to the mobility that can be thought as the energy required to enlarge the radius of an anionic site of length $l(x)$ by an amount δr , the latter quantity being roughly equal to the cation radius:

$$E_m(x) = \frac{1}{2}\pi c_{44}(x)l(x)(\delta r)^2 \quad (0.3)$$

The energy term $E_m(x)$ depends on the shear modulus $c_{44}(x)$ which in turn depends on the Ca concentration [29]. In a floppy model network, the shear modulus $c_{44}(x)$ is zero [25] leading to a zero value for the strain energy $E_m(x)$ and a maximum in mobility.

Additional support for our interpretation derives from two other observations: (1) In the molten $(CaO)_x - (SiO_2)_{1-x}$, we still observe an increase in conductivity with x but with values which are substantially higher compared to the glass (fig. 3) and which can be fitted with a Vogel-Fulcher-Tamman (VFT) law:

$$\sigma T = A \exp[-\Delta/(T - T_0)] \quad (0.4)$$

arising from the variation in temperature of the calcium diffusion constant (via the Nernst-Einstein equation) [26]. From the fits (solid lines in insert of fig. 3) it appears that the pseudo-activation energy Δ is constant for the two values in the floppy region ($\Delta = 2733.0$ and $2740.7K$ for respectively $x = 0.44$ and $x = 0.5$) while it increases for the composition $x = 0.53$ ($\Delta = 3008 K$). Also, the VFT temperature T_0 at which the diffusion constant (and the underlying relaxation time towards thermal equilibrium) diverges is dynamically inaccessible during glass transition, but it is accepted that its value is close to the ideal Kauzmann [27] glass transition temperature T_K . An ideal glass would therefore have its T_g close to T_K and T_0 , a situation which is met in the present system for the Phillips' optimal glass composition $x = 0.5$ ($T_g/T_0 = 1.0002$ compared to $T_g/T_0 = 1.0218$ for $x = 0.44$ and $T_g/T_0 = 1.0621$ for $x = 0.53$).

In fig. 4 are represented the Arrhenius activation energy E_A for conductivity and the preexponential factor σ_0 as a function of the mean coordination number of the network [11] which is $\bar{r} = (8 - 4x)/(3 - x)$. The former displays a minimum at $\bar{r} = 2.4$ which corresponds to $x = 0.5$.

This in turn can be compared to the non-reversing heat flow extracted from complex calorimetric measurements at the glass transition temperature for various chalcogenide systems [30]. Here, this relaxing part of the total heat flow exhibits always a minimum at the floppy to rigid transition (close to the mean-field [10] value $\bar{r} = 2.4$). The same global trend is observed in numerous chalcogenides [30], and our calcium silicate glasses exhibit also a minimum in E_A at the mean coordination number $\bar{r} = 2.4$. From the chalcogenide example, we suggest that when $x = 0.5$ structural relaxation of the glass network proceeds with minimal enthalpic changes because the minuscule network stress is uniformly spread when the network is mechanically critical (i.e. $F/N=0$). Furthermore, we note that the variation of σ is here not driven by the compositional trends of σ_0 . It appears to be rather a balance between the variation of E_A and σ_0 . (2) Rigidity percolation thresholds in Micro-Raman

measurements performed in backscattering geometry have been reported in Ref. [16]. Therefore, we have studied in the present work as a function of the Ca concentration the frequency ν and the linewidth Γ of the stressed rigid $SiO_{4/2}$ (Q^4 unit, where the superscript denotes the number of network bridging oxygens). The corresponding line (A_1 stretching mode) exhibits a change of regime (fig. 5) for the line frequency at the concentration $x = 0.50$, consistently with chalcogen analogs [16]. We concentrate here only on this (stressed rigid) line and will report separately the complete Raman analysis elsewhere [31]. On the other hand, the evolution of the linewidth Γ with x permits to follow the local environnement of the Q^4 unit. For $x < 0.50$, Γ remains constant, related to the absence of change in the coupling of this unit with the rest of the network. It is the coupling which makes possible the presence of rigid regions (through isostatic $Q^4 - Q^3$ and stressed $Q^4 - Q^4$ bondings) although the number of floppy Q^2 and Q^1 units is steadily increasing. Above the critical concentration $x = 0.5$, the sharp drop of Γ clearly shows decoupling of the Q^4 unit with respect to the network (fig. 5), signifying decoupling of stressed rigid regions thus percolation of floppiness.

In FICs, it is often believed that it is the carrier concentration that dominates the conductivity. In the strong electrolyte model [26], the cation electrostatic Coulombic energy barrier has to be overcome to ensure conduction. On the other hand, in the weak electrolyte model a dissociation energy is needed to create the mobile carrier [28]. These two pictures remain of course valid as long as the sizes of the cations is weak compared to the interstices of the glass network.

Our conclusion brings us back to the analogy with alkali oxide FIC's and the popular conductivity channel picture [24]. In these glasses, the rigid to floppy transition occurs at the concentration $x_c = 0.20$ which is very close to the reported threshold concentration separating intrachannel cation hopping (involving a weak mechanical deformation of the network, since the motion occurs only in macroscopic holes of the network) from network hopping (strong mechanical deformation only possible in a floppy network). However, in alkali silicates, no typical behavior emerges in compositional trends of the conductivity be-

cause of the growing contribution of the free carrier rate [24]. This has to be put in contrast with our present study on calcium silicates where the conductivity is almost constant up to a critical value $x_c \simeq 0.48$ beyond which σ steadily increases. Therefore, the free carrier concentration cannot be considered as an increasing function of alkaline earth composition. We believe that conductivity in calcium silicates is driven by the carrier mobility in the network and percolates at the rigid to floppy transition. On this system, further investigations and measurements of physical quantities displaying usually a threshold behavior [33] at the rigidity transition will be achieved in close future.

LPTL is Unité Mixte de Recherche n. 7600. It is a pleasure to acknowledge the help of Boris Robert during the course of this work.

-
- [1] for a review, see *Structure, Dynamics and Properties of Silicate Melts*, J.F. Stebbins, P.F. MacMillan, D.B. Dingwell Eds., Reviews in Mineralogy **32** (1995), Washington DC
 - [2] Ph. Jund, W. Kob, R. Jullien, Phys. Rev. B **64** (2001) 134303.
 - [3] J. Horbach, W. Kob, Philos. Mag. B **79** (1999) 1981.
 - [4] J.D. Frantz, B.O. Mysen, Chem. Geol. **121** (1995) 155.
 - [5] S.S. Kim, T.H. Sanders Jr., J. Am. Ceram. Soc. **82** (1999) 1901.
 - [6] H. Doweidar, J. Non-Cryst. Solids **249** (1999) 194
 - [7] M.K. Eckersley, P.H. Gaskell, A.C. Barnes and P. Chieux, Nature **335** (1988) 525
 - [8] J. Kincs, S.W. Martin, Phys. Rev. Lett. **76** (1996) 70
 - [9] S.W. Martin, Eur. J. Solid St. Inorg. Chem. **28** (1991) 163; P. Boolchand, W. Bresser, Nature **410** (2001) 1070
 - [10] J.C. Phillips, J. Non-Cryst. Solids **34** (1979) 153; M.F. Thorpe, J. Non-Cryst. Solids **57** (1983)

355.

- [11] H. He, M.F. Thorpe, Phys. Rev. Lett. **54** (1985) 2107; W. Bresser, P. Boolchand, P. Suranyi, Phys. Rev. Lett. **56** (1986) 2493.
- [12] J.E. Shelby, J. Appl. Phys. **50** (1979) 8010
- [13] for details of the setup, see M. Malki and P. Echegut, J. Non-Cryst. Solids (2003), in press
- [14] D.K. Belashenko, Inorg. Mater. **32** (1996) 160
- [15] P. Boolchand, Cond. Matt. Sci. **12** (1986) 163.
- [16] P. Boolchand, B. Norban, D. Persing, R.N.ENZWEILER, J.E. Griffiths and J.C. Phillips, Phys. Rev. B **36** (1987) 8109; X. Feng, W.J. Bresser and P. Boolchand, Phys. Rev. Lett. **78** (1997) 4422.
- [17] M. Tatsumisago, B.L. Halfpap, J.L. Green, S.M. Lindsay, C.A. Angell, Phys. Rev. Lett. **64** (1991) 1549
- [18] M. Zhang, P. Boolchand, Science **266** (1994) 1355
- [19] R. Kerner, J.C. Phillips, Solid State Comm. **117** (2000) 47
- [20] T. Taniguchi, M. Okuno, T. Matsumoto, J. Non-Cryst. Solids **211** (1997) 56
- [21] Y. Vaills, G. Hauret, Y. Luspain, J. Non-Cryst. Solids **286** (2001) 224
- [22] L. Pauling, *Die Nature der Chemischen Bindung*, Verlag Chemie, Weinheim, 1962 (Cornell University Press, Ithaca, NY, 1960)
- [23] R. Narayanan, Phys. Rev. B **64** (2001) 134207
- [24] G.N. Greaves and K.L. Ngai, Phys. Rev. B **52** (1995) 6358
- [25] D.S. Franzblau, J. Tersoff, Phys. Rev. Lett. **68** (1992) 2172
- [26] O. Anderson, D. Stuart, J. Am. Ceram. Soc. **37** (1954) 573

- [27] typically $0.9 < T_0/T_K < 1.1$, for a recent review, see P.G. Debenedetti, F. Stillinger, *Nature* **410** (2001) 259
- [28] D. Ravaine, J.L. Souquet, *Phys. Chem. Glasses* **18** (1977) 27
- [29] see for examples: L.F. Perondi, R.J. Elliot, R.A. Barrio, K. Kaski, *Phys. Rev. B* **50** (1994) 9868 or S.R. Elliott, F.E.G. Hehn, *J. Non-Cryst. Solids* **116** (1990) 179
- [30] see for example P. Boolchand, W.J. Bresser, D.G. Georgiev, Y. Wang and J. Wells in *Phase Transitions and Self-Organization in Electronic and Molecular Networks*, Eds. J.C. Phillips, M.F. Thorpe, Plenum Press/Kluwer Academic, New York 2001
- [31] M. Malki, M. Micoulaut, F. Chaimbault, P. Simon, Y. Vaills, in preparation.
- [32] P. McMillan, B. Piriou, *Bull. Mineral.* **106** (1983) 57
- [33] For a review on Raman, calorimetric, etc. studies related to rigidity transitions, see *Rigidity theory and applications*, Ed. M.F. Thorpe, P.M. Duxburry, Plenum Press/Kluwer Academic, New York 1999

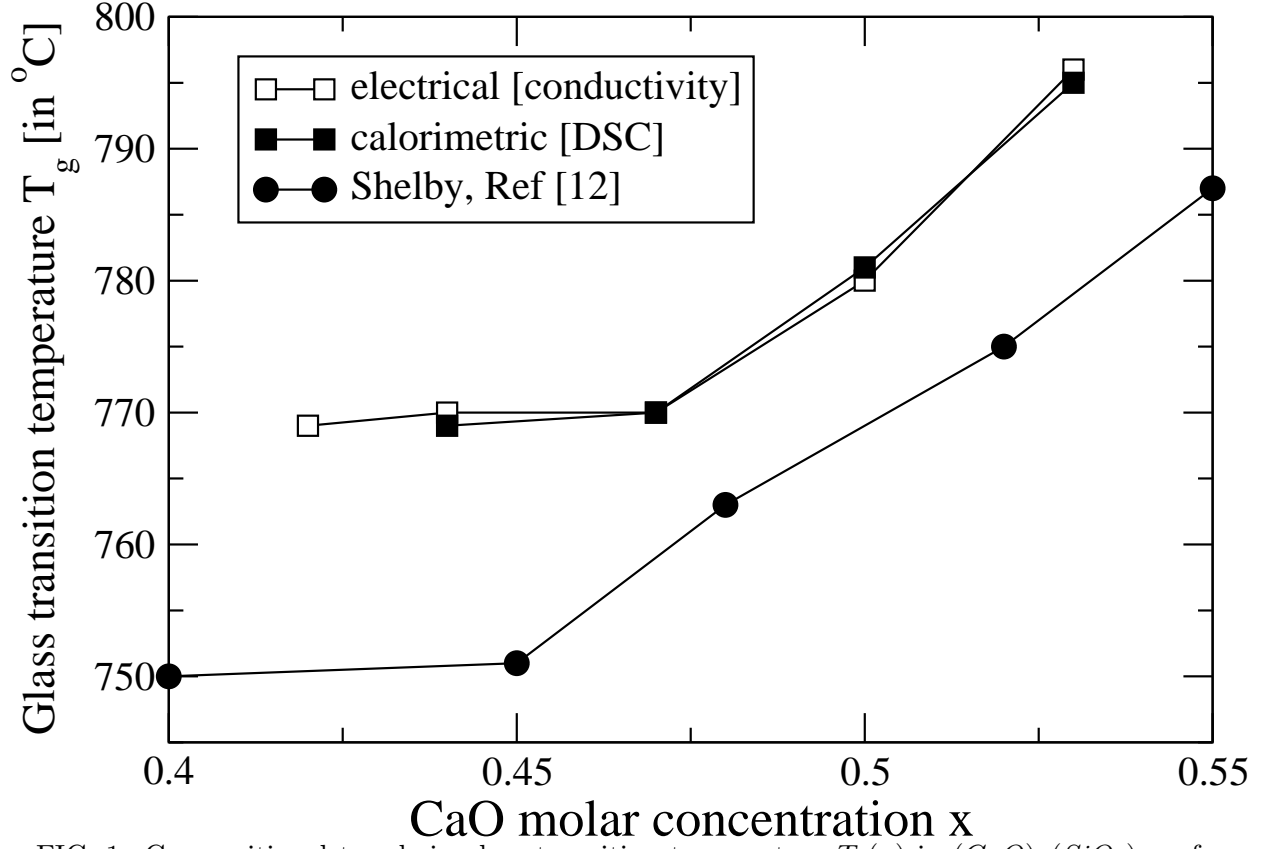


FIG. 1. Compositional trends in glass transition temperature $T_g(x)$ in $(CaO)_x(SiO_2)_{1-x}$ from DSC and electrical measurements, compared to previous studies[12]

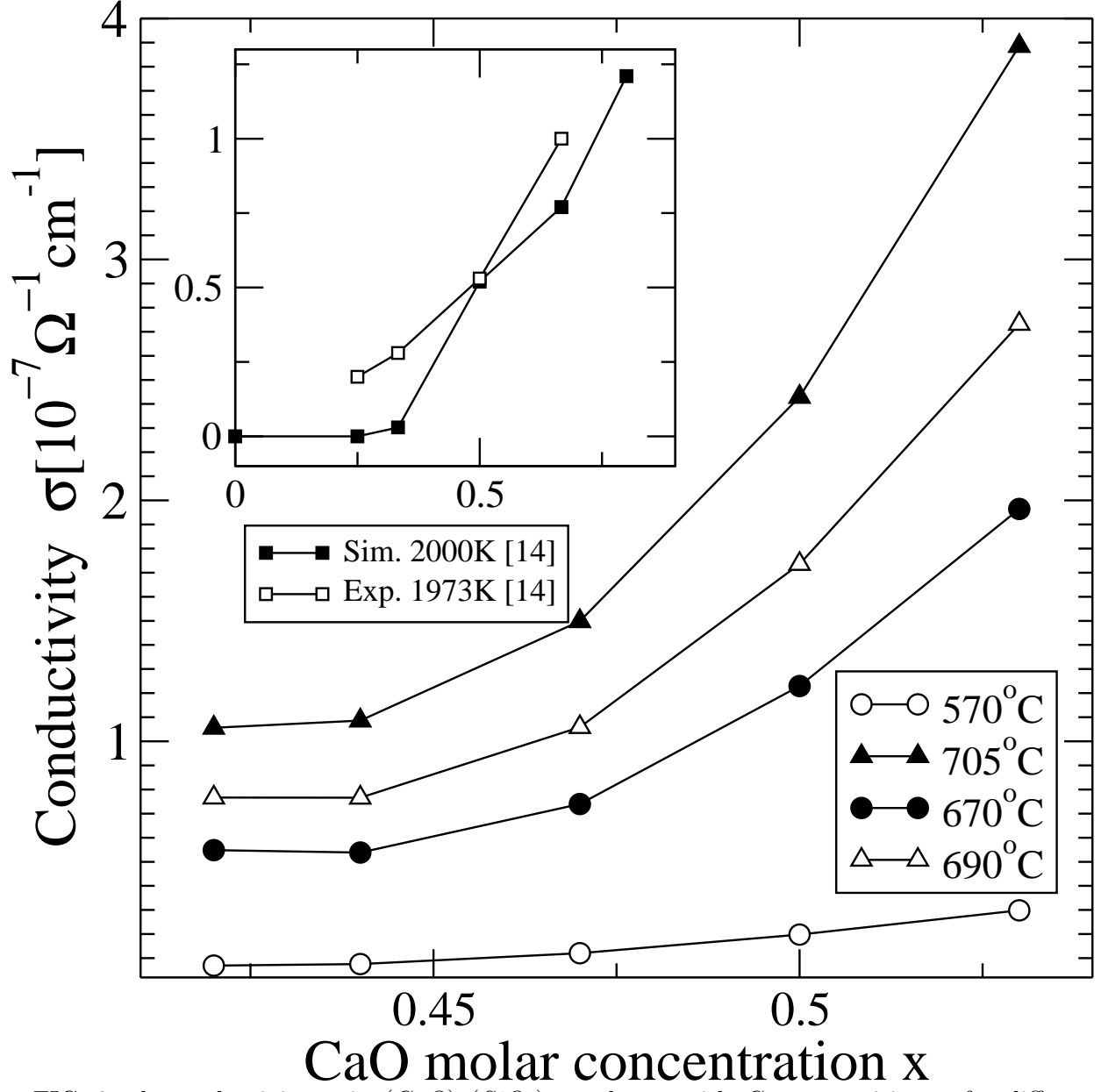


FIG. 2. dc conductivity σ in $(\text{CaO})_x(\text{SiO}_2)_{1-x}$ glasses with Ca composition x for different temperatures. The insert shows the conductivity in the melt from simulation and previous experiments[14] at around 2000 K .

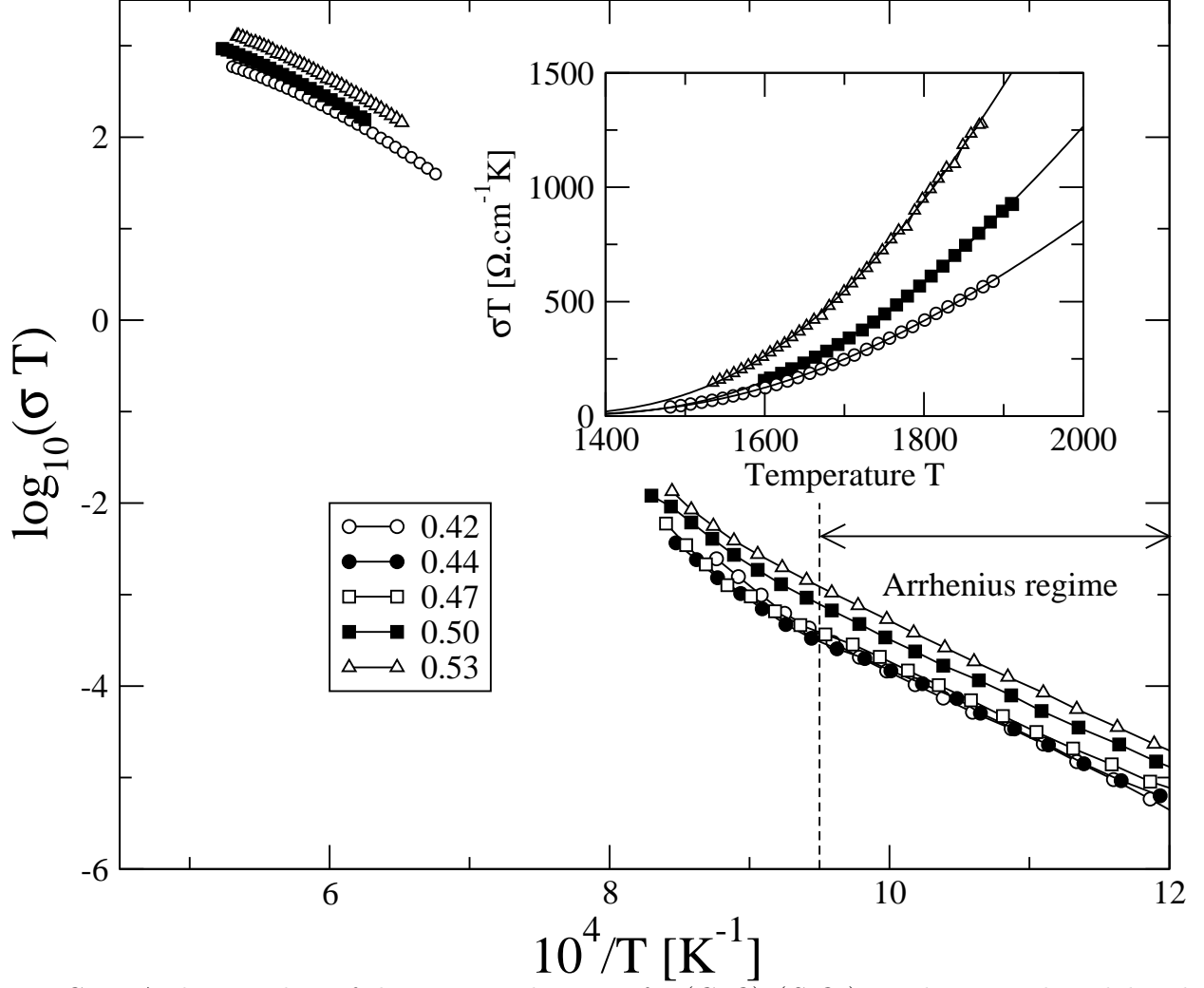


FIG. 3. Arrhenius plots of the ionic conductivity for $(CaO)_x(SiO_2)_{1-x}$ glasses in the solid and the molten state. The fit for the estimation of E_A and σ_0 have been performed at low temperature in the Arrhenius regime. Note the small deviation occurring close to the glass transition temperature. The insert shows σT in the liquid as a function of temperature with corresponding Vogel-Fulcher-Tamman (VFT) fits.

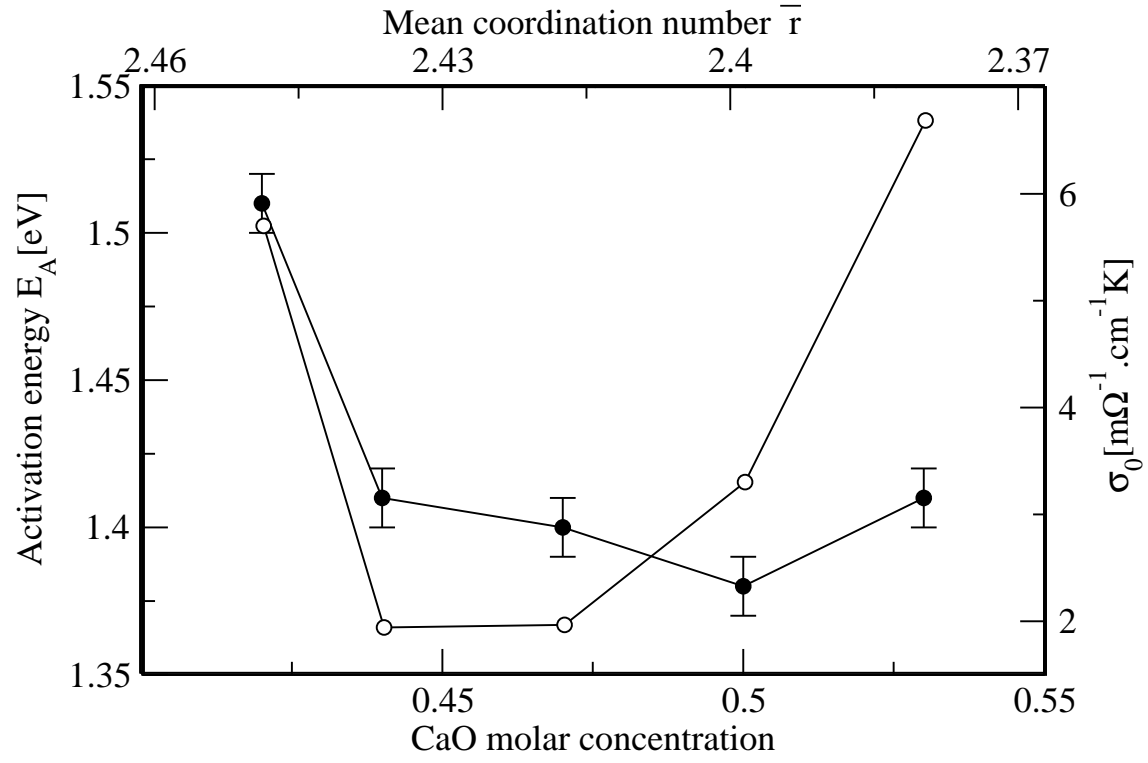


FIG. 4. Arrhenius parameters (activation energy E_A (solid circles) and preexponential factor σ_0 (open circles)) as a function of the mean coordination number \bar{r} in the glass phase.

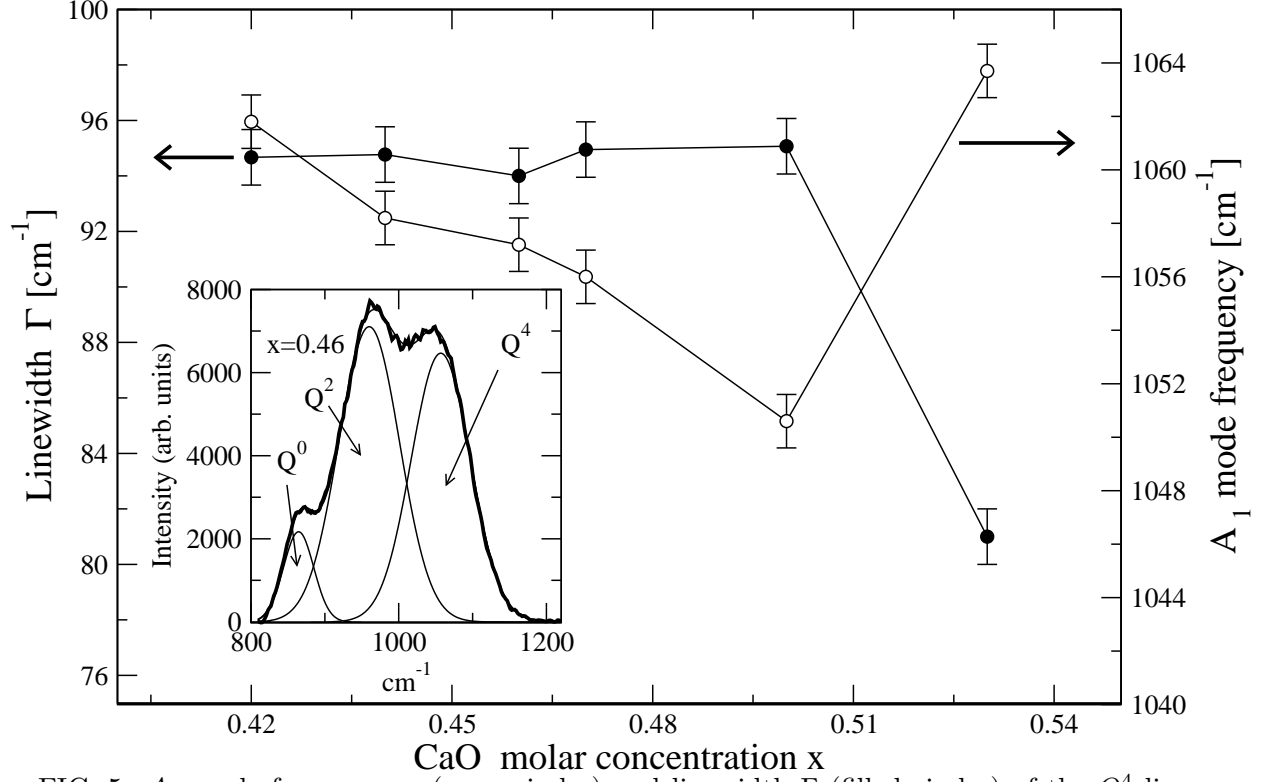


FIG. 5. A_1 mode frequency ν (open circles) and linewidth Γ (filled circles) of the Q^4 line as a function of Ca concentration. The insert shows part of the Raman spectra with the line of interest for $x = 0.46$ and the related Gaussian fits at 850 cm^{-1} [Q^0 unit] and 950 cm^{-1} [Q^2 unit] from [32].